

Magnetic Resonance Imaging of Suspicious Ovarian Lesions

Thesis

Submitted for Partial Fulfilment of Master Degree In
Radio-Diagnosis

By

Asmaa Hamdy Ahmed

M.B.B.Ch Faculty of Medicine - Ain Shams University (2012)

Supervised by

Dr. Ayman Mohammed Ibrahim

*Assistant Professor of Radiology
Faculty of Medicine, Ain Shams University*

Dr. Amgad Samy Abdel-Rahman

*Lecturer of Radiology
Faculty of Medicine, Ain Shams University*

**Faculty of Medicine
Ain Shams University
2018**



Acknowledgement

*First of all, all gratitude is due to **Allah** almighty for blessing this work, until it has reached its end, as a part of his generous help, throughout my life.*

*Words can never express my feelings and gratitude to my **Professor Dr. Ayman Mohammed Ibrahim**, Assistant Professor of Radio-diagnosis, Faculty of medicine, Ain Shams University, for his continuous care, support and for his patience, supervision and guidance throughout the whole work,*

*Special thanks to **Dr. Amgad Samy Abdel Rahman**, Lecturer of Radio-diagnosis, Faculty of medicine, Ain Shams University for his guidance and great effort during this study.*

*I want to express my respect and appreciation to **Dr. Hossam El Kholi** and **Dr. Ahmed Hussein** for their attendance.*

*I would like to express my respect and internal appreciation towards my big family especially **my Mother** who has always been there for me and for her continuous praying, everlasting love and care.*

*Special thanks to my small family especially **my Husband** who was always been there for me thanks for your encouragement and real great support.*



Asmaa Hamdy Ahmed

List of Contents

	Page
Acknowledgment	--
List of abbreviations	i
List of tables	iii
List of figures	iv
Introduction	1
Aim of the Work	3
Review of literature:	4
• Radiological anatomy of female pelvic organs	4
• Pathology of ovarian lesions.....	12
• Technique of MRI.....	30
• MRI findings of ovarian lesions	43
Patients and methods	94
Results	100
Discussion	109
Illustrative cases	113
Summary and conclusion	126
References	127
Arabic summary	--

List of Abbreviations

ADC	Apparent Diffusion Coefficient
AFP	Alpha fetoprotein
CCC	Clear cell carcinoma
CE	Contrast Enhanced
CSF	Cerebro spinal fluid
CT	Computerized tomography
DCE-MRI	Dynamic Contrast Enhanced Magnetic Resonance Imaging
DWI	Diffusion Weighted
FIGO	International Federation of Gynecology and Obstetrics
FOV	Field Of View
FSE	Fast Spin Echo
HCG	Human chorionic gonadotrophin
LDH	Lactate dehydrogenase
LN	Lymph Node
MRI	Magnetic Resonance Imaging
MRS	Magnetic resonance spectroscopy
NPV	Negative predictive value
PCO	Polycystic ovary
PID	Pelvic inflammatory disease
PPV	Positive predictive value
RF	Radio frequency
ROC	Recessive operating characteristics
ROI	Region Of Interest
SD	Standard deviation

List of Abbreviations (Cont.)

SI	Signal intensity
SNR	Signal to noise ratio
T	Tesla
T2WI	T2- weighted image
TE	Time echo
THRIVE	T1 high resolution isotropic volume
TIC	Time intensity curve
TIWI	T1 weighted image
TOA	Tubo-ovarian abscess
TR	Time of repetition
TVUS	Trans-vaginal ultrasound
US	Ultrasound

List of Tables

Table	Title	Page
1	Pathological classification of ovarian lesions.	12
2	Pathological classification according to cell of origin.	13
3	Epidemiology of ovarian tumors.	23
4	Staging of cancer ovary.	25
5	TNM classification of cancer ovary.	27
6	Summary of typical imaging features of ovarian lesions.	92
7	Different pathological types of examined cases.	100
8	Minimum & maximum diameters of examined lesions.	101
9	Different morphological features of examined lesions.	101
10	Side of examined lesions.	102
11	ADC values of examined lesions.	105
12	Cutoff values of benign vs malignant lesions.	106
13	Relation of TIC to pathology.	107
14	Pattern of enhancement of examined lesions.	108

List of Figures

Fig.	Title	Page
1-5	Normal MRI anatomy of female pelvis.	6-11
6	Gross specimen of serous cystadenoma.	15
7	Gross specimen of serous cystadenofibromas.	15
8	Gross specimen of high grade serous carcinoma.	15
9	Gross specimen of mucinous cystadenoma.	16
10	Gross specimen of mucinous carcinoma.	16
11	Gross specimen of clear cell carcinoma.	17
12	Gross specimen of mature cystic teratomas.	18
13	Gross specimen of yolk sac tumor.	19
14	Gross specimen of immature teratomas.	20
15	Gross specimen of granulosa cell tumor.	21
16	Physics of MRI.	31
17	Preparation before MRI.	34
18	MRI of typical dermoid.	43
19	MRI of functional cyst.	45
20	MRI of hemorrhagic cyst.	45
21	MRI of TOA.	46
22	MRI of mucinous cystadenoma.	47
23	Papillary projections in mucinous cystadenoma.	48
24	MRI of cystadenofibroma.	49
25	MRI of mature cystic teratoma.	50
26	MRI of struma ovarii.	52
27	MRI of ovarian thecoma.	54
28	MRI of ovarian fibroma.	54
29	MRI of brenner tumor.	55

Fig.	Title	Page
30	Light bulb sign of endometrioma.	57
31	MRI of endometrioma.	58
32	MRI of endometrioma.	59
33	Shading sign of endometrioma.	60
34	MRI of endometrioma.	61
35	Kissing ovaries.	62
36	MRI of endometrioma.	63
37-38	DWI &ADC of endometrioma.	64
39	Polycystic ovary.	65
40	Paraovarian cyst.	66
41	Peritoneal inclusion cyst.	66
42&43	Ovarian torsion.	68
44	Twisted ovarian teratoma.	69
45	Ovarian torsion.	70
46	High grade ovarian cystadeno-carcinoma.	71
47	Borderline serous cystadenoma.	72
48	Mucinous adenocarcinoma.	73
49	Mucinous borderline tumor.	74
50	Malignant transformation of endometrioma.	75
51	Endometroid carcinoma.	76
52	Clear cell carcinoma.	77
53	Indeterminate CCC.	78
54	Endometrioma with CCC.	78
55	Clear cell adenofibroma associated with CCC.	79
56	Proliferating brenner tumor.	80
57	Granulosa cell tumor.	81
58	Solid form of granulosa cell tumor.	82
59	Poorly differentiated sertoli-leydig tumor.	83

Fig.	Title	Page
60	Dysgerminoma .	84
61	Immature teratoma.	85
62	Malignant transformation of mature teratoma.	85
63	Ovarian choriocarcinoma.	86
64	Yolk sac tumor.	87
65	Ovarian lymphoma.	88
66	Bilateral ovarian lymphoma.	89
67	Krukenburg tumor.	91
68	Time intensity curves.	98
Chart1	Pathological classification of examined cases	100
Chart2	Signal intensity characteristics of examined lesions.	104
Chart3	Different types of TIC.	107
Chart4	Relation of TIC to pathological diagnosis.	108

Introduction

Ovarian masses are a common finding in daily clinical practice and may be incidentally detected or identified in symptomatic patients. Characterization of an ovarian lesion represents a diagnostic challenge; it is of great importance in the preoperative setting in order to plan adequate therapeutic procedures and may influence patient's management. The optimal assessment of an adnexal mass requires a multidisciplinary approach, based on physical examination, laboratory tests and imaging techniques. Preoperative biopsy should not be performed in ovarian masses, particularly if the mass appears to be surgically resectable at the moment, as this invasive procedure raises the risk of spreading cancer cells worsening the prognosis so, diagnostic imaging plays a crucial role in detection, characterization and staging of adnexal masses (*Foti et al., 2016*).

Magnetic Resonance Imaging (MRI) is an essential problem solving tool to determine the site of origin of a pelvic mass and then to characterize an adnexal mass, especially in patients with indeterminate lesions (*Chilla et al., 2011*).

The main advantages of MRI are the high contrast resolution with excellent soft tissue contrast and lack of ionizing radiation exposure, which is particularly important in young female patients (*Chilla et al., 2011*). Magnetic resonance imaging (MRI) can produce images that are not only exquisite in structural details but can also provide

functional information in tumors (*Kauppinen and Peet, 2011*).

Magnetic resonance imaging, MRI, provides high spatial resolution, such that morphology is very well visualized. With the aid of magnetic resonance imaging (MRI), adnexal masses with morphologic characteristics that are indeterminate on trans-vaginal ultrasound can sometimes be better identified as benign or malignant (*Belkić and Belkić, 2017*).

Aim of The Work

The aim of the study is to evaluate role of magnetic resonance imaging as a powerful and noninvasive technique which may effectively characterize and differentiate between various suspicious ovarian lesions.

RADIOLOGICAL ANATOMY OF THE FEMALE PELVIC ORGANS

Female pelvic anatomy is elegantly demonstrated by MRI. On T2WI, the uterus typically demonstrates three distinct layers: high-intensity endometrium, low-intensity junctional zone, and intermediate-intensity outer myometrium. If there is fluid within the uterine cavity, it is seen as high signal intensity on a T2-weighted image, which is indistinguishable from the endometrium. The junctional zone represents inner myometrium (*Jung and Kim, 2012*).

During menstruation or the premenarchal and postmenopausal periods, the zonal architecture of the uterine corpus may be indistinct. The myometrium commonly demonstrates homogeneous delayed enhancement. The junctional zone may demonstrate lower signal intensity than the outer myometrium on contrast-enhanced sequences. The endometrium enhances later and often stays higher in signal intensity on delayed contrast-enhanced images than the myometrium (*Jung and Kim, 2012*).

The cervix commonly shows similar zonal anatomy as the uterine corpus on T2WI. The inner stroma shows lower signal intensity than the outer stroma. As in the junctional zone of the uterine corpus, the inner cervical stroma is histologically composed of compact cells with more nuclei than the outer stroma. In some cases, however, the whole cervix is seen as having low signal intensity on T2WI. On contrast-enhanced MRI, the cervix often enhances similarly to the myometrium. Not infrequently, however, it enhances later and less intensely than the myometrium (*Jung and Kim, 2012*).

Lateral to the uterus there is a prominent uterine and parametrial vascular plexus. These are seen as very high T2, low T1 signal intensity serpiginous structures. In the normal state, flow through these vessels is slow and hence seen as high T2 signal intensity. In states of high flow, signal voids are seen on both T2 and T1 signal intensity (*Sahdev, 2013*).

Most of the supporting ligaments of the uterus are well demonstrated on MRI. The round ligament is seen as a low T2 signal intensity cord projecting anteriorly from the cornu toward the internal inguinal ring and into the inguinal canal. It terminates by inserting diffusely into the mons pubis. The lateral uterine and cervical ligaments (cardinal ligaments) and uterosacral ligaments are seen as strands of low T2 signal intensity anchoring the uterine body and cervix to the lateral pelvic wall and sacrum, respectively. Strands of uterosacral ligaments also merge into the perirectal fascia. The broad ligament is a peritoneal reflection encompassing the round ligament, fallopian tubes and venous plexus but cannot be seen as a distinct structure on MRI (*Sahdev, 2013*).

On MRI, normal ovaries can be identified best on T2-weighted images between the uterine cornu and the pelvic side wall. On T1-weighted images, the ovaries have a homogenous intermediate T1 signal intensity. The ovaries lie in the hollow between the origins of the internal and external iliac arteries. These may be found more superiorly if previously displaced by a gravid uterus, fibroids, or pelvic surgery. In premenopausal women, ovarian stroma has intermediate T2 signal intensity but may demonstrate high T2 signal intensity varying with menstrual phase. The ovaries are easily identified by the presence of multiple follicles of high T2 signal intensity. Following administration of gadolinium, ovarian stroma enhances avidly but less than myometrium. In post- menopausal

women, ovaries contain very few, if any, follicles and the stroma has intermediate T2 signal intensity with little enhancement after gadolinium administration. Normal fallopian tubes are not seen on MRI or TVUS (*Sahdev, 2013*).

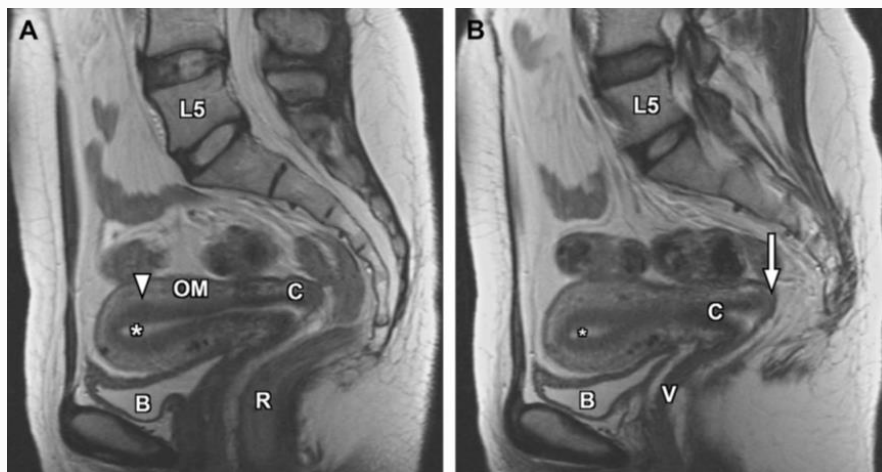


Fig.1: Sagittal T2-weighted images of the female pelvis in midline (A) and Para midline (B) locations. The zonal anatomy of the uterus is well demonstrated on T2-weighted images, with high signal intensity in the endometrium (asterisk) and characteristic low signal intensity of the junctional zone (arrowhead). Outer myometrium demonstrates intermediate signal intensity between the two other uterine layers. The cervix is well seen in longitudinal dimension, noting contiguity of the dark fibromuscular stroma with the uterine junctional zone. The posterior fornix (arrow) is formed from the posterior reflection/interface of the exocervix and the vagina. B, bladder; C, cervix; L5, L5 vertebral level; OM, outer myometrium; R, rectum; V, vagina (*Wasnik et al., 2011*).